ICOLD 75th Annual Meeting
Saint Petersburg, Russia, June 24-29, 2007

Symposium: «Dam Safety Management. Role of State, Private Companies and Public in Designing, Constructing and Operating of Large Dams»

EXPERIMENTAL INVESTIGATION OF DYNAMIC UPLIFT IN CONCRETE GRAVITY DAM

Shigeki Uruchida[1], Yoshinori Yagome[2], Katsutoshi Kubota[3], Yoshihisa Uchita[4] and Victor Saouma[5]

ABSTRACT Dynamic uplift in dams is not yet fully understood, and various organizations have adopted different models. To address this unresolved problem, tests have been performed on a dam model mounted on a shaking table inside a centrifuge. Hence, this paper will report on the experimental determination of dynamic uplifts.

In these tests, a 70-cm-high model of a concrete gravity dam, along with the accompanying reservoir is subjected to a 30 g vertical acceleration (thus the prototype height is 21 m). Once the desired g level has been reached, the dam model is subjected to a series of harmonic excitations of increasing amplitudes. This excitation induced the occurrence of an upstream crack and its subsequent propagation. The harmonic excitation had a frequency of 194 Hz, which corresponds to 6 Hz in the actual prototype.

Since the dam was in full contact with the reservoir, water penetrated the crack, and both crack opening displacements as well as internal uplift pressures were recorded. Pressure transducers connected to small external holes intersecting the crack trajectory measured uplift.

The experiments showed that dynamic pressure was inversely proportional to crack openings. Furthermore, if the crack opening is sufficiently large, then there was full water penetration, on the other hand for very small crack openings, we observed negative pressure, or cavitations, as the viscosity of the water compounded by the roughness of the crack hindered full water penetration into the newly generated crack/void.

BACKGROUND

Analysis assumptions of various organizations Different organizations have different analysis assumptions on how to model earthquake-induced uplift pressures along a crack. Javanmardi (2002) identified the following assumptions (see Table 1):

• The International Commission on Large Dams, ICOLD (1986), assumes that a capillary water pressure equivalent to the reservoir head immediately penetrates the crack.

• The US Army Corps of Engineers (1995), the Federal Energy Regulatory Commission (2002) assume

that uplift pressures in cracks or joints are not influenced by earthquakes.

• The Bureau of Reclamation, USBR (1987) assumes that the uplift pressure in the crack is zero. " when a crack develops during an earthquake event, uplift pressure within the crack is assumed to be zero. This assumption is based on studies that show the opening of a crack during an earthquake relieves internal water pressure, and the rapidly cycling nature of opening and closing the crack does not allow reservoir water, and the associated pressure, to penetrate."

• The Canadian Dam Safety Agency (1997) assumes that in weak-earthquake areas, pre-quake uplift pressures remain constant during an earthquake even in seismically induced cracks. Furthermore, even in areas of strong-seismicity uplift pressures remains zero even in the presence of crack openings.

Table 1 Assumptions on earthquake-induced uplift along the crack (Javanmardi et al.)

	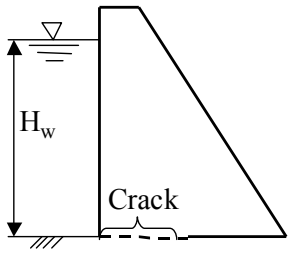
Initial uplift distribution	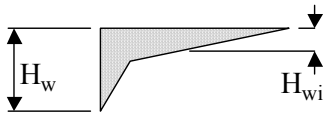
Full uplift pressure is attained in seismic cracks (ICOLD1986)	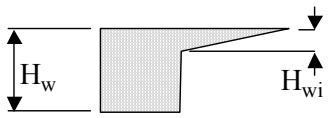
Uplift pressure in existence crack and joint unchanged during the earthquake (USACE1995, FERC2002, CDSA1997 low seismic zone)	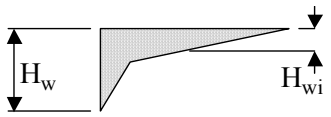
・ Uplift pressure is reduced to zero during the earthquake (USBR1987) ・ Uplift pressure is reduced to zero or unchanged during the earthquake (CDSA1997, high seismic zone)	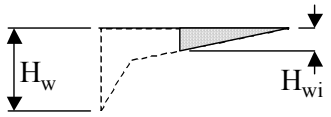

Previous studies Javanmardi et al. (2002) conducted an experiment on a cracked concrete column. In the experiment, internal water pressures of 10 to 500 kPa were applied to a crack, which opening varied between 0.2 and 2.0 mm through harmonic oscillations of 2, 6 and 10 Hz. Water pressure was measured at five locations.

Slowik and Saouma (2000) used a wedge splitting test apparatus to induce crack propagation and measured water pressures along the crack while the water pressures acted on the crack opening. They pointed out that during crack closure water might not be completely expunged; hence it acts as a wedge inducing large tensile stresses on the "downstream" side.

Omachi et al. (1998) conducted a shaking table experiment to investigate dynamic water pressures within cavities. They prepared an acrylic cavity model with a crack opening of 0.15 to 1.0 cm and a cavity depth of 30 cm, placed the model in an underwater shaking table, and measured dynamic water pressure while the model was submerged in the water to a depth of 10 cm. The experiment showed that dynamic water pressure tended to increase linearly in proportion to the distance from the crack mouth and also revealed trends of changes under the influence of frequency and crack opening.

Purpose of this study The authors are developing the nonlinear finite element analysis program MERLIN (Saouma et al.). In previous benchmark study, the authors conducted a centrifuge shaking table test on a concrete dam model mimicking a dam and reservoir and then performed the numerical simulation with MERLIN to track crack generation and growth. In a previous analysis of an arch gravity dam, Shimpo et al. used also MERLIN to determine the imminent failure flood (IFF) by considering the effect of uplift along a crack. This experimental study is conducted to investigate dynamic water pressures with the crack by performing centrifuge shaking table test of a dam model with a crack in contact with the water storage. This purpose aims considering dynamic uplift on dynamic analysis using MERLIN.

TEST METHOD The dam model, shown in Fig.1, is placed in a steel container (1,500 mm long, 400 mm wide, 725 mm deep) so that the upstream side can be impounded the dam body (500 mm high) and its foundation (50 mm high) are both made of mortar.

Table 2 shows the mix proportions of the mortar, and Table 3 shows the mechanical properties evaluated by the laboratory test conducted on cylindrical samples with the same age as the mortar used for the dam model. In a preliminary test conducted prior to the test, the dam model was subjected to 194 Hz harmonic excitations in the stream direction in a 30g gravity field to cause a crack at an acceleration of about 500 m/s^2. To facilitate the initiation of the crack, an initial notch was cut at the upstream surface. Crack propagation was then monitored indirectly through the crest acceleration response and strain at the surface of the dam model.

Table 2 Mix Proportion

W/(C+FA) (%)	FA/B (%)	Mass of unit volume (kg/m^3)			
		W	B		Sand Surface dry
			C	FA	
70	40	240	206	137	1527
Air entraining and water reducing agent (kg/m^3)					27

Table 3 Mechanical Properties of the Specimen (62days)

Compressive strength (N/mm^2)	11.8
Young's modulus (10^4 N/mm^2)	1.173
Poisson's ratio	0.185
Tensile strength (N/mm^2)	1.283
Unit weight (kg/m^3)	2017
Fracture energy (N/mm)	0.049

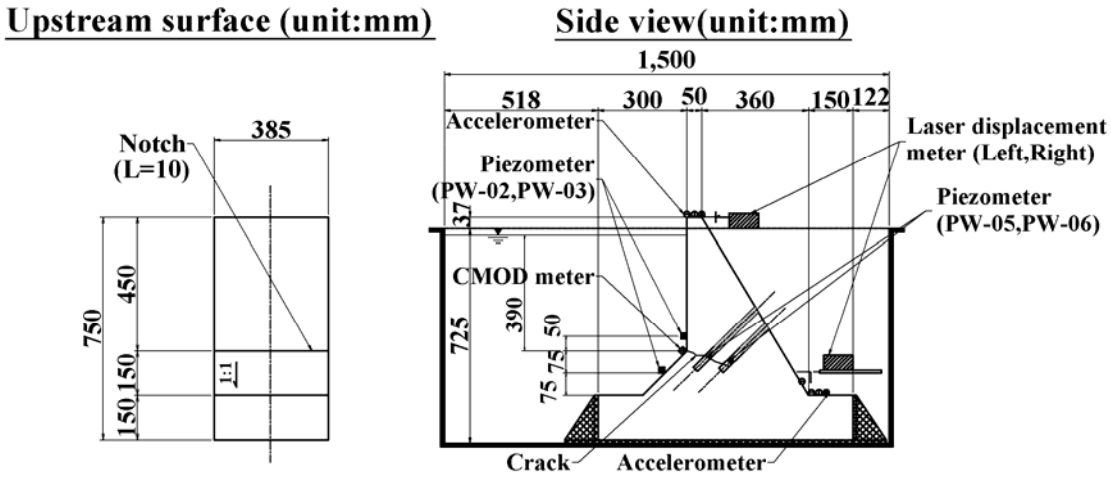

Fig.1 Shape of Specimen and Arrangement of Monitoring Device

Fig.2 shows the initial crack in the preliminary test and the arrangement of the piezometers used. Due to acceleration in the dam axis direction, the crack trajectory is not perfectly symmetric between the right and left sides; instead, it is triangular. Water pressure was measured at two locations: at a point in the cracked region on the right side for the purpose of measuring water pressure acting on the existing crack and at a point on the left side outside the cracked region for the purposes of comparison and of measuring water pressure response in a newly formed crack during the main test. The measuring instruments were installed as follows. After the preliminary test, the dam model was taken out of the container, two 20 mm diameter holes were bored from the downstream face of the dam to depths below the crack depth, a piezometer was connected to each borehole. The space around each piezometer was filled with saturated sand, and each hole was filled again with grout. In order to prevent water absorption from the borehole wall, a glycol-ether concrete curing agent was applied to the borehole wall several times, and it was verified that no water was being absorbed from the borehole wall.

In the excitation test, twelve steps of harmonic excitation (referred to as S1 to S12), in which the maximum bedrock acceleration was varied from 50 m/s^2 to 500 m/s^2, and small-white-noise excitation with a maximum bedrock acceleration of 15 m/s^2 were alternated.

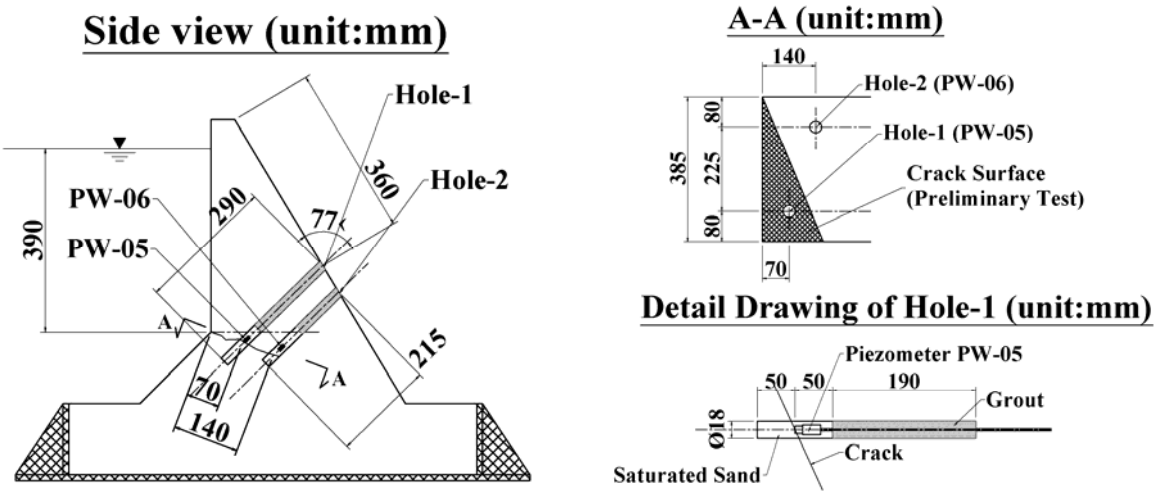

Fig.2 The way of installing the piezometers and the arrangement plan

TEST RESULTS

Overview Table 4 shows the maximum bedrock acceleration measured at the dam foundation for each excitation step. Fig.3 shows the crack observed after the test. As shown, on both the right and left sides, the crack that occurred at the corner between the two slopes propagated until it approached the downstream face of the dam. Based on the crack mouth opening displacements (CMOD) and the relative crest displacements versus the bedrock in the stream direction, shown in Fig.4, and the changes in dominant frequency of the specimen shown in Fig.5, it is speculated that the crack grew considerably in or around the S10 excitation. All strain gauges that had been attached to both sides of the model for the preliminary test were removed in order to improve the seal between the dam and the container. There was a concern that the thickness of the gages and of the wires would hamper the perfect seal between dam and container specially that the dam was subjected to hydrostatic pressure of 21 m. The dynamic water pressures measured on the upstream face of the dam model show fair agreement with the calculated values obtained from the Westergaad equation (Fig.6).

Table 4 Ground Accelerations for Each Excitation

Excitation No.	Acceleration (m/s^2) Target / Recorded	Excitation No.	Acceleration (m/s^2) Target / Recorded
S1	25 / 8	S7	400 / 415
S2	50 / 61	S8	400 / 412
S3	100 / 107	S9	500 / 485
S4	200 / 239	S10	500 / 519
S5	300 / 310	S11	500 / 496
S6	400 / 350	S12	500 / 481

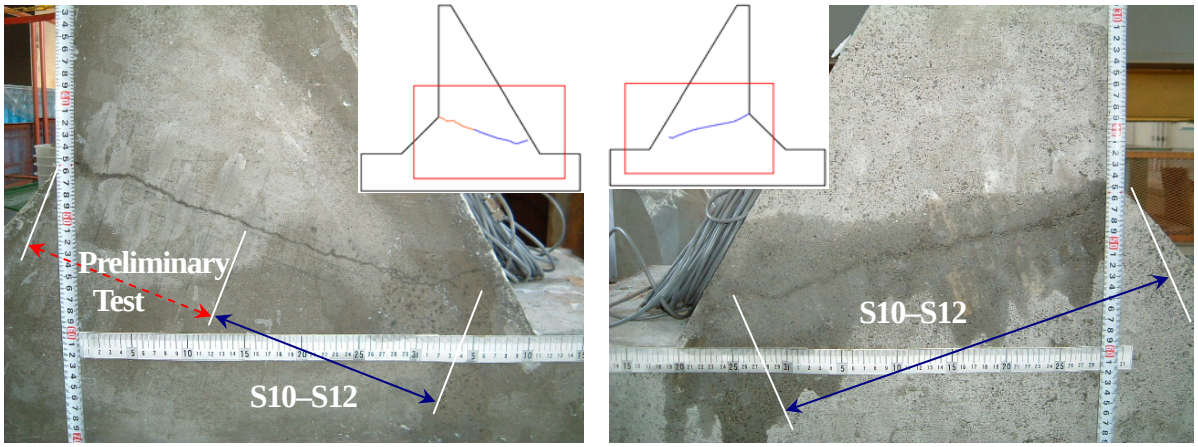

(a) Right face (b) Left face

Fig.3 The Cracks in the Specimen

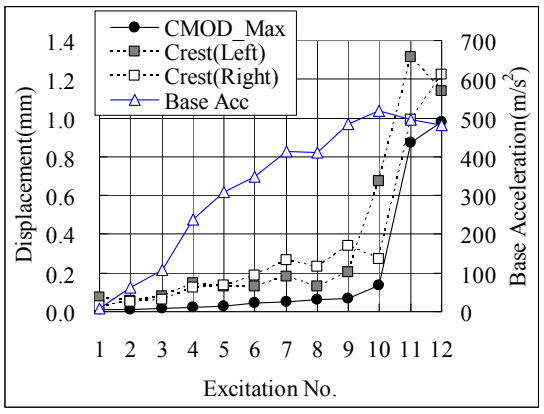

Fig.4 CMOD and Crest Displacements

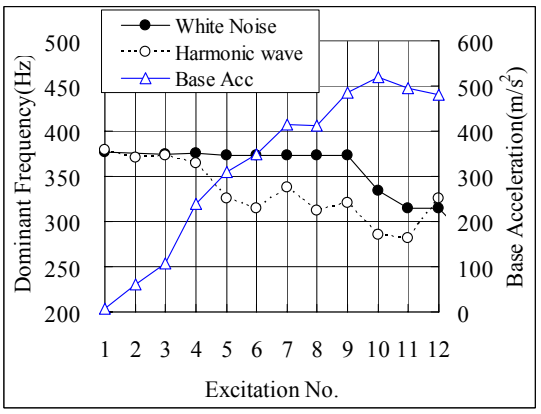

Fig.5 Dominant frequency

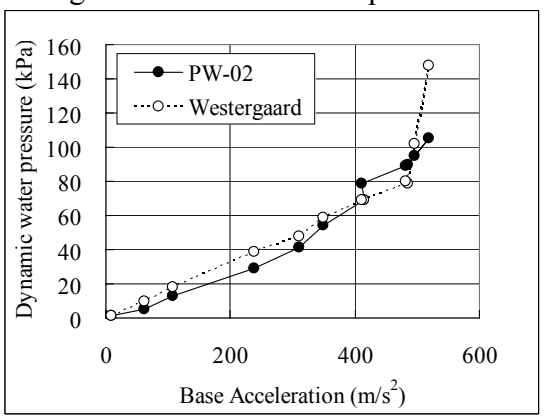

(a) Fillet part

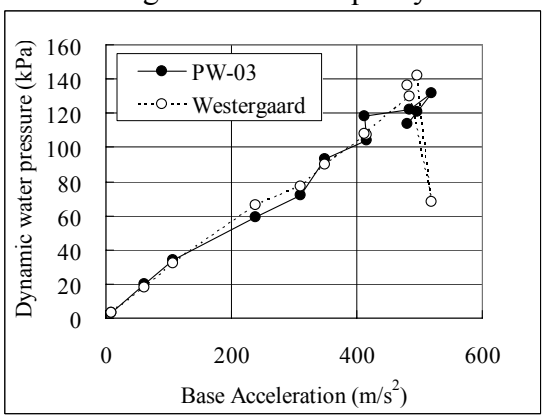

(b) Vertical wall surface part

Fig.6 Dynamic water pressure on upstream surface

Fig.7 illustrates the measured water pressures in the crack at each excitation step. Fig.7 (a) shows the initial water pressure before the excitation, and Fig.7 (b) shows the maximum water pressure observed during excitation. It is speculated that at or soon after S10 that the crack became fully saturated with reservoir water. This is further confirmed by the fact that at S10 maximum water pressure started to dramatically increase. The fact that different maximum water pressures were observed during excitation at the right and left sides is consistent with the fact that the response displacement on the right side tends to be greater than that on the left one.

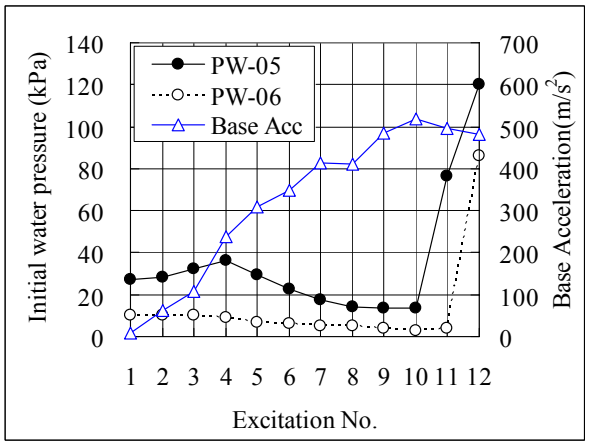

(a) Initial pressure

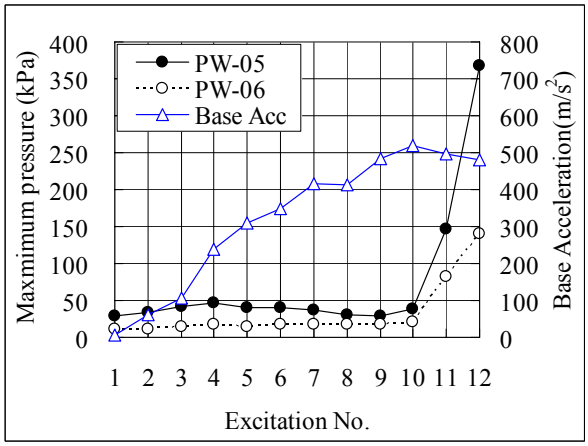

(b) Maximum pressure

Fig.7 The changed of water pressure in crack

Classification of water pressure response patterns Water pressures in the crack exhibited the four patterns described below. Table 5 shows a typical waveform of each pattern and the corresponding excitation number.

Table 5 The Classification of the dynamic water pressure response

Pattern	Water Pressure and CMOD (Time Historical)	Schematic Diagram	Excitation No.	
			PW-05	PW-06
I	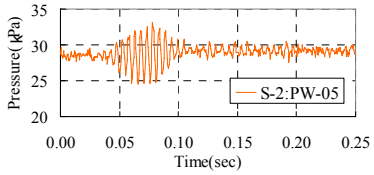	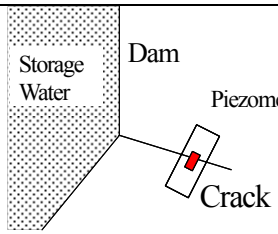	S1-S3	S1-S10
II	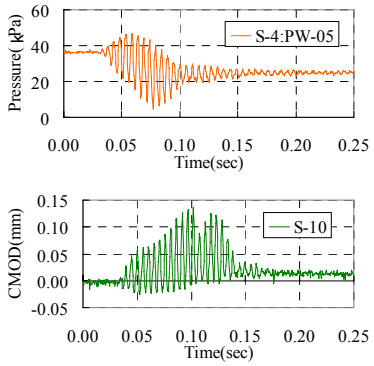	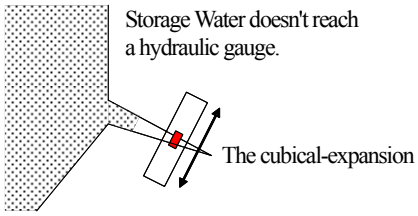	S4-S10	S11
III	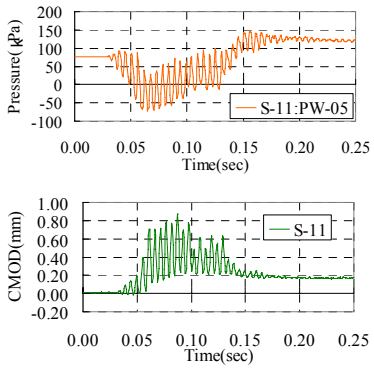	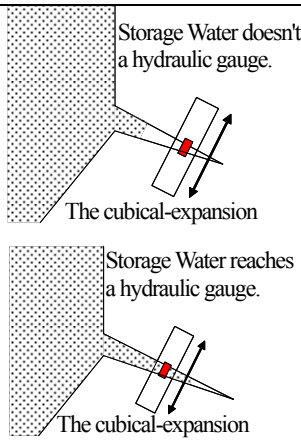	S11	S12
IV	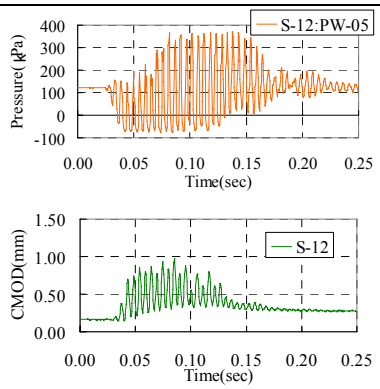	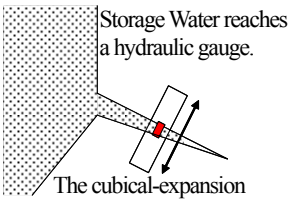	S12	-

Pattern I (right side: S1–S3, left side: S1–S10) The initial water pressure before the excitation ranges from 10 to 40 kPa. In terms of hydraulic head, these values roughly correspond to the length of the water pressure measurement hole. The water pressure amplitude during excitation is 10 kPa or less, and there is no residual water pressure after excitation. As shown in Fig.8, water pressure and crack opening displacement (CMOD) are in opposite phases. From these characteristics, it can be inferred that at this stage the crack opening is too small and the storage water has not penetrated into the crack, and that the changes in water pressure have been caused by changes in the volume of the measurement hole due to dam body deformation instead of interaction with the reservoir.

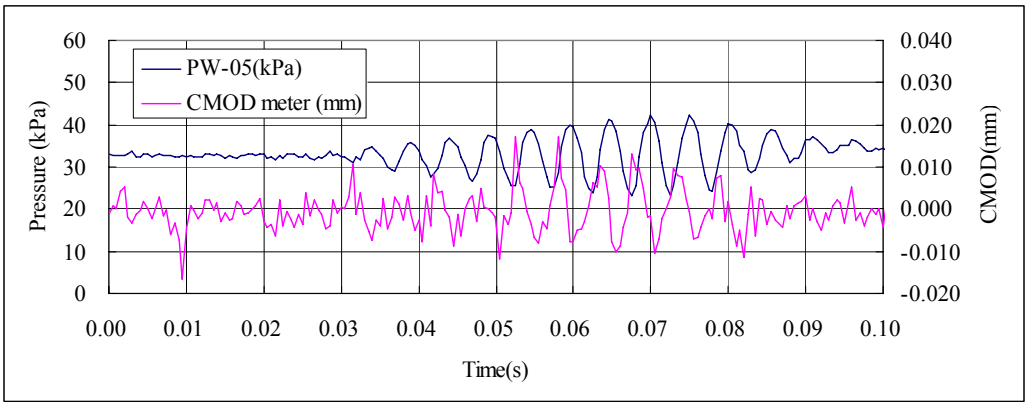

Fig.8 Water Pressure and CMOD

Pattern II (right side: S4–S10, left side: S11) Water pressure amplitudes are proportional to crack opening and range from about 40 to 50 kPa. This is slightly larger than in Pattern I amplitudes. Water pressure decreased from the initial water pressure, and there was residual water pressure after excitation. As in Pattern I, water pressure and crack opening displacement are again in opposite phases. Although small crack openings occurred at the piezometer location, water penetration has not yet started, and it can be inferred that negative pressure has been accumulated. During the excitation at S10, residual crack opening displacement after excitation increased noticeably and reached about 0.01 mm.

Pattern III (right side: S11, left side: S12) Residual displacement increased to 0.17 at S11and to 0.28 mm at S12. Factors contributing to these results are thought to include the complex shape of the crack and spalls from the crack surfaces. The fact that water pressure increased during excitation is thought to indicate that storage water intruded into the crack and saturation occurred. Crack opening displacement reached about 0.9 mm, and the water pressure amplitudes were about 100 kPa, which were even greater than in Pattern II amplitudes. Although water pressure decreased because of negative pressure in the first half of the excitation, it subsequently increased in the second half, and the residual water pressure after excitation was greater than the initial water pressure. In the second half of the excitation, the water reached the piezometer location. It is thought likely that the crack grew during excitation. The acceleration response was unstable, and frequency disturbances occurred.

Pattern IV (right side: S12, left side: not applicable) The water pressure amplitudes are similar to those shown in Pattern II and Pattern III results. The water in the crack reached the piezometer location. Residual crack opening displacement became more noticeable. The piezometer measurements directly

reflect reservoir water pressures, and water pressure and crack opening displacement are in opposite phases.

Fig.9 (a) and 9(b) show the crack mouth opening displacements (CMOD) and crack mouth opening velocities (CMOV) during the S12 excitation, along with water pressure time histories. There are phase differences between the CMOD and water pressure peaks, and water pressure increased and peaked while the crack was closed. On the other hand, the phase difference between the CMOV and water pressure peaks are antiphase. The maximum and minimum values of water pressure occurred during the CMOV peaks while the crack was closed and open respectively. Fig.10 and Fig.11 show the water pressures during the S12 excitation in terms of the relationship between CMOD and CMOV. Because the duration of excitation is short and the water pressure response is transient, the water pressures have been plotted layer by layer in the five time zones (i) to (v) shown in Fig.9 (a). The open-crack results are shown in green, and the closed-crack results are shown in orange. The data form counterclockwise loops. This tendency is particularly pronounced in (i) to (iii), which show large crack opening amplitudes. In these figures, the loop diameter becomes larger with time. On the negative pressure side, water pressure plateau at the saturated vapor pressure. In Fig.10 (iv) to (v), which shows results in the latter half of the excitation process, water pressure decreases as the crack opening amplitude becomes smaller. The relationship between water pressure and CMOV is almost linear on the closed-crack side (+) and the open-crack side (−), respectively, and the slopes of the plots become steeper (which means an increase in water pressure) with the progress of saturation.

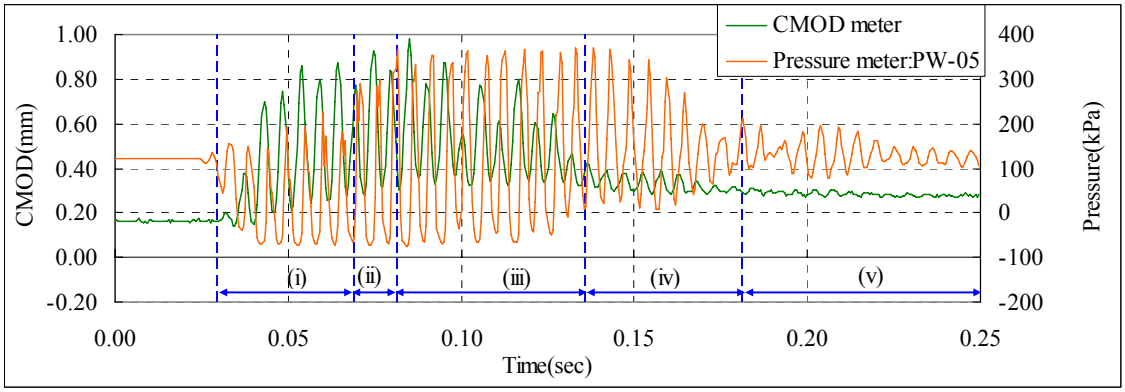

(a) CMOD and Water Pressure

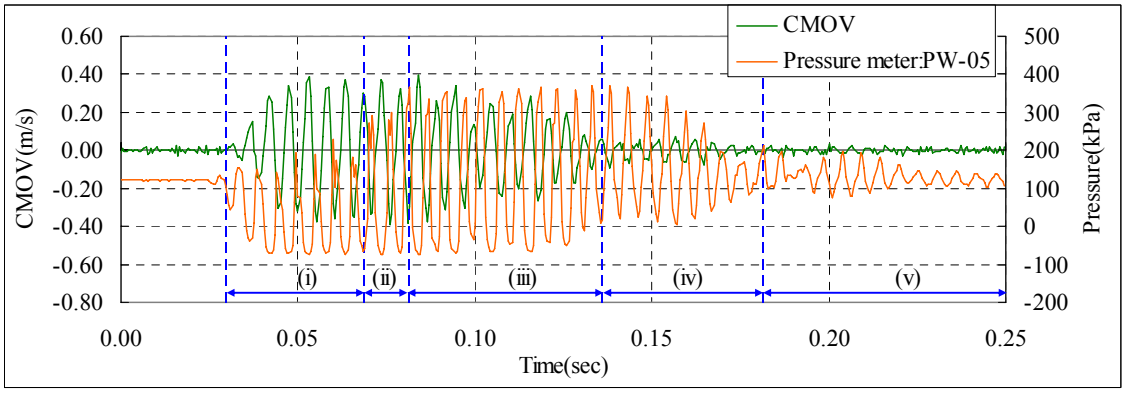

(b) CMOV and Water pressure

Fig.9 CMOD, CMOV and Water pressure During S12 Excitation

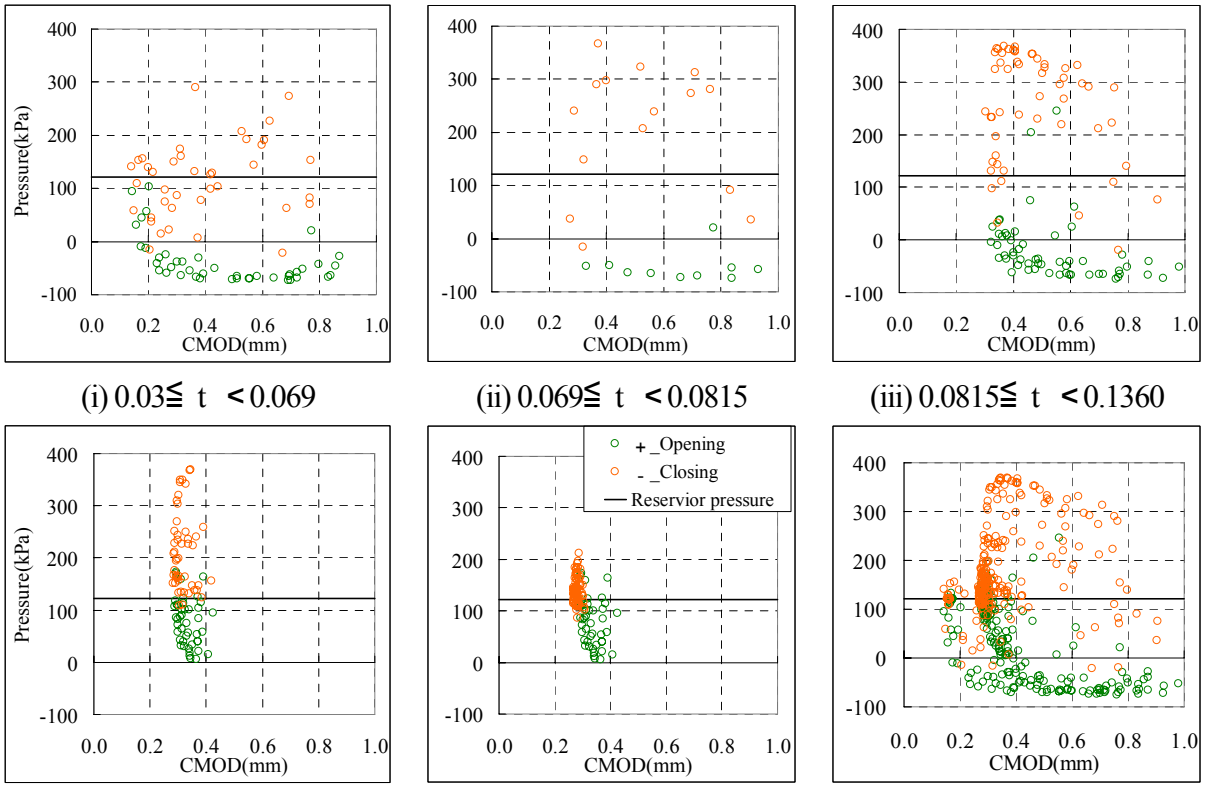

(i) 0.03≦ t <0.069 (ii) 0.069≦ t <0.0815 (iii) 0.0815≦ t <0.1360

(iv) 0.1360≦ t <0.1815 (v) 0.1815≦ t <0.250 (vi) All data

Fig.10 The Relationship between Water Pressure and CMOD

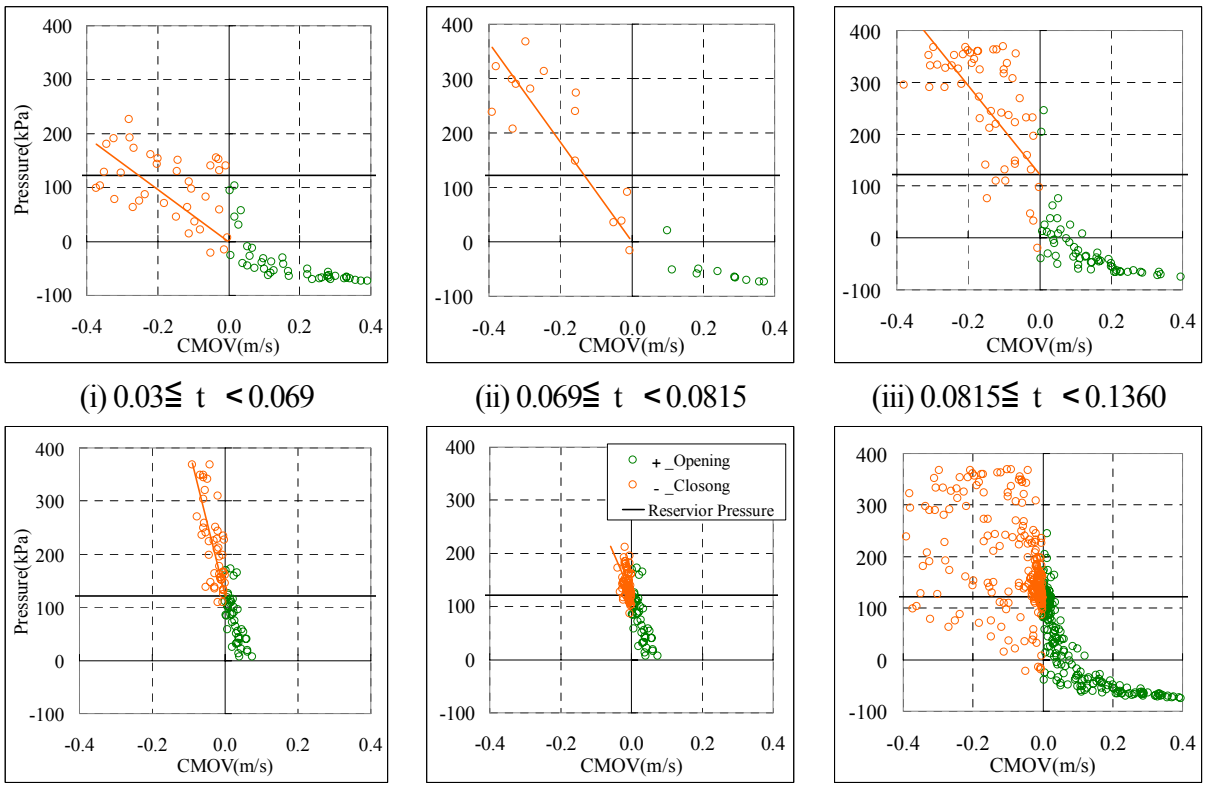

(i) 0.03≦ t <0.069 (ii) 0.069≦ t <0.0815 (iii) 0.0815≦ t <0.1360

(iv) 0.1360≦ t <0.1815 (v) 0.1815≦ t <0.250 (vi) All data

Fig.11 The Relationship between Water Pressure and CMOV

CONCLUSION Based on this investigation, we conclude that:

• By exciting a dam model in the stream wise direction, a crack first occurred, and then propagated, while the dynamic uplift pressure was recorded.

• During crack opening, water would flow inside the crack, however the crack surface roughness compounded with the water viscosity might have limited the inflow. This resulted in cavitations at the tip of the crack, a region not infilled with water.

• Tests indicated that after the crack opening became large enough to permit the full penetration of storage water inside the entire crack length, the water pressure was recorded with relatively good accuracy in terms of the CMOV. This indicates dynamic uplift could and should be accounted for in dynamic non-liner analysis through this relationship.

In the test conducted for the purposes of this study, the shape of the crack was complex, and it was difficult to control parameters such as crack opening and crack opening velocity. The authors are currently conducting water pressure experiments using a simple crack model with an opening–closing mechanism consisting of two concrete plates and are trying to apply computational fluid dynamic (CFD) analysis techniques in order to directly model water pressure phenomena in an open or closed crack.

REFERENCES

Javanmardi, F., Leger, P., Tinawi, R. Experimental Measurements of Water Pressure in Concrete Cracks Due to Seismic Loading. 4th Structural Specialty Conference of the Canadian Society for Civil Engineering (2002) Paper ST-014

Ohmachi, T., Zhang, H., Yabuki, N.,Tsukada, N. Experimental Study of Hydrodynamic Pressure Inside Narrow Cavities. Dam Engineering, Japan Society of Dam Engineers, No.8, No.1 (1998) 35-40

Shimpo, T., Uchita, Y., Saouma, V.E., Full Non Linear Analysis of an Arch Gravity Dam Using MERLIN. ICOLD 7th Benchmark Workshop, Romania (2003) 104-118

Slowik, V., Sauma, V.E., Water Pressure in Propagating Concrete Cracks. Journal of Structural Engineering Feb. 2000, ASCE (2000) 235-242

Uruchida, S., Shimpo, T., Uchita, Y., Yagome, Y., Saouma, V.E., Dynamic Centrifuge Tests of Concrete Gravity Dam. 73rd Annual Meeting of ICOLD Tehran, Iran (2005) Paper No.085-04

[1] Dam Group, Construction Engineering Center, Tokyo Electric Power Co., Inc.
[2] Dept. of Hydraulic Power Engineering, Tokyo Electric Power Services Co., Inc.
[3] Dam Group manager, Construction Engineering Center, Tokyo Electric Power Co., Inc.
[4] Specialist, Construction Engineering Center, Tokyo Electric Power Co., Inc.,
[5] Professor, Department of Civil, Environmental and Architectural Engineering, University of Colorado in Boulder